



## BUCKLING ANALYSIS OF SKEW PLATES SUBJECTED TO UNIFORM COMPRESSION LOADING

Budiman<sup>1</sup>

<sup>1</sup>Civil Engineering Study Program, University of Muhammadiyah Jakarta, Jl. Cempaka Putih Tengah 27, Indonesia

Correspondence email: budiman30@umj.ac.id

Received December 15, 2021 | Accepted January 19, 2022

### ABSTRACT

*The main objective of the research work is to present the buckling analysis of plates subjected to uniform compressive load. To obtain accurate results in analysis plate must be free from shear locking, this phenomenon occurs when the ratio of length to thickness ratios plate increases. Many investigations have been carried out on plate elements to see the behavior of a plate in the case of thin plates. In this paper, we investigated plate analysis in the case of buckling analysis using one of the finite element plates, the numerical analysis was conducted on a skew plate with varying length to thickness ratios, and skew angles. The reference solution in the literature will be used to compare the analysis results the level of convergence and plate performance will be obtained.*

**Keywords:** Buckling; Critical buckling load; Skew plate; Finite element.

### 1. INTRODUCTION

One of the tools used to analyze plate elements is the finite element method, The finite element method is a numerical method that uses discretization techniques on elements by dividing a part of the finite whole into small pieces, which are interconnected only at nodal points. If an element formulation cannot discretize the element accurately then a shear locking occurs, this phenomenon occurs when length to thickness ratios ( $L/h$ ) increases [1].

The plate must be able to eliminate the shear effect when the length to thickness ratios ( $L/h$ ) increases, this is done to qualify as a Kirchhoff plate. Plate analysis results will not be accurate when the plate element

depends on its thickness which causes shear locking. Many researchers propose approaches to overcome the shear effect, one of which is MITC3 (3-node triangular mixed interpolation of tensorial components) developed by Lee & Bathe [2]. MITC3 plate element was developed through the "mixed interpolation of tensorial components" (MITC) concept, plate elements based on this approach have been able to give good results on quadrilateral elements [3],[4].

The development and research of the MITC3 element can be found in [1],[2], and [5]. Research on buckling analysis using the finite element method has been carried out [6]-[7]. In this paper, to show the performance and convergence behavior of

MITC3, we conducted a buckling analysis of the skew plate using MITC3 with varying length to width ratios ( $L/h$ ), and skew angle ( $\theta$ ). Reference solutions from the literature were then used to validate the results.

## 2. REISSNER-MINDLIN PLATE THEORY

### Strain-Displacement Equation

According to Reissner-Mindlin plate first-order shear deformation plate theory [9], the displacement field can be declared as:

$$\begin{aligned} u(x, y, z) &= u(x, y) + z\beta_x(x, y) \\ v(x, y, z) &= v(x, y) + z\beta_y(x, y) \\ w(x, y, z) &= w(x, y) \end{aligned} \quad (1)$$

where  $u$ ,  $v$ , and  $w$  are displacements of the mid-plane of the plate,  $\beta_x$  and  $\beta_y$  represent the rotations of the transverse normal about the  $x$  and  $y$  axes, respectively.

The linear strains are given by:

$$\begin{Bmatrix} \epsilon_{xx} \\ \epsilon_{yy} \\ \gamma_{xy} \end{Bmatrix} = \begin{Bmatrix} \beta_{x,x} \\ \beta_{y,y} \\ \beta_{x,y} + \beta_{y,x} \end{Bmatrix} = z \{\chi\} \quad (2)$$

$$\begin{Bmatrix} \gamma_{yz} \\ \gamma_{xz} \end{Bmatrix} = \begin{Bmatrix} \beta_x + w_{,x} \\ \beta_y + w_{,y} \end{Bmatrix} = \{\gamma\} \quad (3)$$

The notation of  $\beta_{x,x}$  and  $\beta_{y,y}$  state the first derivatives with respect to  $x$  and  $y$  respectively of  $\beta_x$ ,  $w_{,x}$  and  $w_{,y}$  are the first derivatives with respect to  $x$  and  $y$  respectively of vertical displacement  $w$ .

### Constitutive Equations

According to hook law's the stress in the plane can be declared as:

$$\{\sigma\} = [E]\{\epsilon\} \quad (4)$$

The shear stress is as follows

$$\{\tau\} = [G]\{\gamma\} \quad (5)$$

The constitutive equations can be simplified as:

$$\begin{Bmatrix} \sigma_x \\ \sigma_y \\ \tau_{xy} \end{Bmatrix} = \frac{E}{1-\nu^2} \begin{bmatrix} 1 & \nu & 0 \\ \nu & 1 & 0 \\ 0 & 0 & \frac{(1-\nu)}{2} \end{bmatrix} \begin{Bmatrix} \epsilon_x \\ \epsilon_y \\ \gamma_{xy} \end{Bmatrix} \quad (6)$$

$$\begin{Bmatrix} \tau_x \\ \tau_y \end{Bmatrix} = \frac{E}{2(1+\nu)} \begin{bmatrix} 1 & 0 \\ 0 & 1 \end{bmatrix} \begin{Bmatrix} \gamma_{yz} \\ \gamma_{xz} \end{Bmatrix}$$

Where the matrix of material is:

$$\begin{aligned} [E] &= \frac{E}{1-\nu^2} \begin{bmatrix} 1 & \nu & 0 \\ \nu & 1 & 0 \\ 0 & 0 & \frac{(1-\nu)}{2} \end{bmatrix} \\ [G] &= \frac{k E}{2(1+\nu)} \begin{bmatrix} 1 & 0 \\ 0 & 1 \end{bmatrix} \end{aligned} \quad (7)$$

The notation of  $E$  declares the modulus of elasticity,  $\nu$  is Poisson's ratio, and  $k= 5/6$  is the shear correction factor.

## 3. THE FORMULATION OF MITC3 PLATE ELEMENT

MITC3 is the element proposed by Lee and Bathe, this element is based on the concept of "mixed interpolation of tensorial components" (MITC) by Dvorkin and Bathe [4] which uses the tying points to get the shear strain matrix.

MITC3 element has 3 nodes with 3 degrees of freedom for each node, namely:  $w_i$  (translation in the  $z$ -direction)  $\beta_{xi}$  (rotation in the  $z$ - $x$  plane), and  $\beta_{yi}$  (rotation in the  $z$ - $y$  plane).

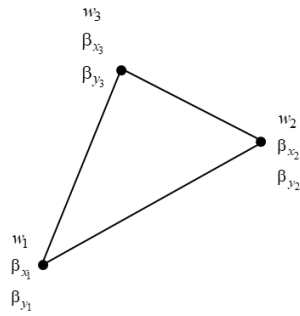


Figure 1. MITC3 elements with 3 nodes and 3 dof per node.

Independent rotation field  $\beta_x$  and  $\beta_y$  and displacement  $w$  are declared as:

$$\begin{aligned}
 w &= \sum_{i=1}^3 N_i w_i \\
 \beta_x &= \sum_{i=1}^3 N_i \beta_{x_i} \\
 \beta_y &= \sum_{i=1}^3 N_i \beta_{y_i}
 \end{aligned} \tag{8}$$

Where  $N_i$  is the linear shape function at node-i.

$$\begin{aligned}
 N_1 &= 1 - \xi - \eta \\
 N_2 &= \xi \\
 N_3 &= \eta
 \end{aligned} \tag{9}$$

### The Bending Strain for MITC3

The relationship between nodal variables and curvature  $\{\chi\}$  is:

$$\{\chi\} = [B_b] \{u_n\}$$

$$[B_b] = \begin{bmatrix} 0 & N_{i,x} & 0 \\ \dots & 0 & N_{i,y} \dots \\ 0 & N_{i,y} & N_{i,x} \end{bmatrix}_{i=1,2,3} \tag{10}$$

### The Shear Strain for MITC3

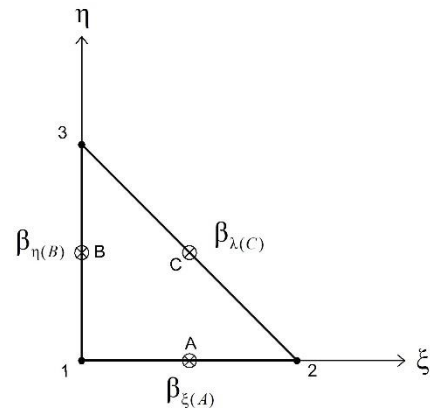


Figure 2. Tying point

The tying point is chosen in the mid-points of sides 1-2, 1-3, and 2-3. Distribusi  $\beta_\xi$  is assumed constant  $\xi$  and  $\beta_\eta$  is assumed constant along  $\eta$ .

$$\begin{aligned}
 \beta_\xi &= a_1 + a_2 \eta \\
 \beta_\eta &= b_1 + b_2 \xi \\
 \beta_\lambda &= \frac{1}{\sqrt{2}} (\beta_\xi - \beta_\eta)
 \end{aligned} \tag{11}$$

The value of  $\beta_\xi$  and  $\beta_\eta$ , at the tying points, is the average of the values for each corner of the side, then:

$$\begin{aligned}
 \beta_{\xi(A)} &= \frac{1}{2} (\beta_{\xi_1} + \beta_{\xi_2}) \\
 \beta_{\eta(B)} &= \frac{1}{2} (\beta_{\eta_1} + \beta_{\eta_3}) \\
 \beta_{\xi(C)} &= \frac{1}{2} (\beta_{\xi_2} + \beta_{\xi_3}) \\
 \beta_{\eta(B)} &= \frac{1}{2} (\beta_{\eta_3} + \beta_{\eta_3})
 \end{aligned} \tag{12}$$

Hence, the shear strain matrix as below;

$$\begin{aligned}
 [B_s] &= [j][B_{s_\xi}] = \begin{bmatrix} [B_{s_1}] & [B_{s_2}] & [B_{s_3}] \end{bmatrix} \\
 [B_{s_1}] &= \frac{1}{4A} \begin{bmatrix} -y_{13} & -y_{21} \\ x_{13} & x_{21} \end{bmatrix} \\
 &\begin{bmatrix} -2 & (x_{21} + x_{32}\eta) & (y_{21} + y_{32}\eta) \\ -2 & -(x_{13} + x_{32}\xi) & -(y_{13} + y_{32}\xi) \end{bmatrix} \\
 [B_{s_2}] &= \frac{1}{4A} \begin{bmatrix} -y_{13} & -y_{21} \\ x_{13} & x_{21} \end{bmatrix} \\
 &\begin{bmatrix} 2 & (x_{21} + x_{32}\eta) & (y_{21} + y_{32}\eta) \\ 0 & -x_{13}\xi & -y_{13}\xi \end{bmatrix} \\
 [B_{s_3}] &= \frac{1}{4A} \begin{bmatrix} -y_{13} & -y_{21} \\ x_{13} & x_{21} \end{bmatrix} \\
 &\begin{bmatrix} 0 & x_{21}\eta & y_{21}\eta \\ 2 & -(x_{13} + x_{21}\xi) & (y_{13} + y_{21}\xi) \end{bmatrix}
 \end{aligned} \tag{13}$$

**The Shear Strain for MITC3**

The total energy due to bending and shear can be stated as:

$$\Pi_{int} = \Pi_{int}^b + \Pi_{int}^s \tag{14}$$

Where  $\Pi_{int}$ ,  $\Pi_{int}^b$ , and  $\Pi_{int}^s$  are internal, bending, and shear energy respectively.

The total stiffness due to bending, and shear can be expressed as:

$$[k] = [k_b] + [k_s] \tag{15}$$

Where

$$\begin{aligned}
 [k_b] &= \int_A [B_b]^T [H_b] [B_b] dA \\
 [k_s] &= \int_A [B_s]^T [H_s] [B_s] dA
 \end{aligned} \tag{16}$$

**4. BUCKLING ANALYSIS**

in the case of buckling, the thing to be achieved is to get the value of the critical buckling load due to the application of the load and the buckling mode. Getting it can be solved through the eigenproblem [10]:

$$([k] - N_{cr} [k_G]) \{d\} = \{0\} \tag{17}$$

Where,

$[k]$  = Structural Stiffness Matrix

$N_{cr}$  = Critical buckling load

$[k_G]$  = Geometric stiffness matrix

$\{d\}$  = mode shape

**Matriks kekakuan geometri**

The internal energy equation for membrane deformation is

$$\Pi_\sigma = \frac{1}{2} \langle u_n \rangle [k_G] \{u_n\} \tag{18}$$

The nodal displacement vectors

$$\langle u_n \rangle = \langle w_1 \quad \beta_{x1} \quad \beta_{y1} \quad w_2 \quad \beta_{x2} \quad \beta_{y2} \quad w_3 \quad \beta_{x3} \quad \beta_{y3} \rangle \tag{19}$$

The geometric stiffness matrix is as follows

$$\begin{aligned}
 [k_G] &= h \int_A [G_w]^T [\sigma_0] [G_w] dA \\
 &+ \frac{h^3}{12} \int_A [G_{\beta_x}]^T [\sigma_0] [G_{\beta_x}] dA \\
 &+ \frac{h^3}{12} \int_A [G_{\beta_y}]^T [\sigma_0] [G_{\beta_y}] dA
 \end{aligned} \tag{20}$$

**5. NUMERICAL ANALYSIS**

Numerical analysis was carried out on the fully modeled skew plate that was supported by clamped ( $w=0$ ,  $\beta_x=0$ , and  $\beta_y=0$ ) on each side, the plate was subjected to a uniform compressive uniaxial in-plane load. In this research, the skew plate will be analyzed using variations in length to thickness ratio of  $L/h = 100$  and  $L/h = 1000$ . The analysis was performed using variations in mesh size ( $N \times N \times 2$ ) of  $4 \times 4 \times 2$ ,  $8 \times 8 \times 2$ ,  $16 \times 16 \times 2$ ,  $32 \times 32 \times 2$ , the element was analyzed at several variations of skew angle of  $45^\circ$ ,  $60^\circ$ ,  $75^\circ$ . Validating plate convergence ( $L/h=100$ ) due to compressive uniaxial load, critical buckling load is given by Kumar et al [7].

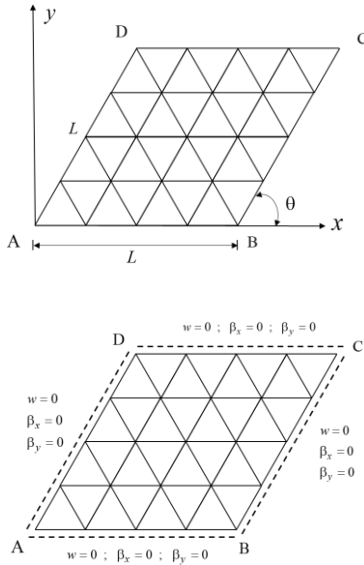


Figure 3. The modeling of the skew plate with CCCC boundary conditions.

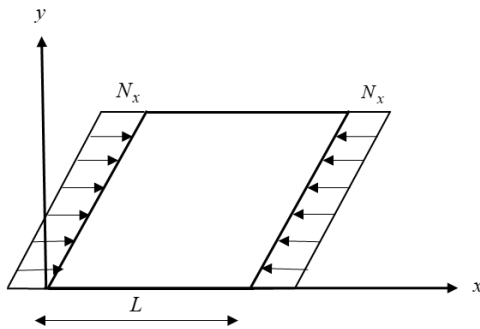


Figure 4. The geometry of plates under uniform compressive load.

Table 1. Critical buckling load  $N_{cr}$  of CCCC skew plate with  $L/h=100$ .

$N \times N \times 2$	Mode number	Skew angle $\theta$		
		$\theta = 45^\circ$	$\theta = 60^\circ$	$\theta = 75^\circ$
$32 \times 32 \times 2$	1	5.080	7.675	9.502
	2	5.572	8.651	10.922
	3	8.930	14.230	18.275
	4	9.647	16.556	23.088
	5	12.642	19.619	23.963
Kumar et al. Error! Reference source not found.]	1	5.110	7.612	9.431

Table 2. Critical buckling load  $N_{cr}$  of CCCC skew plate with  $L/h=100$ .

$N \times N \times 2$	Mode number	Skew angle $\theta$		
		$\theta = 45^\circ$	$\theta = 60^\circ$	$\theta = 75^\circ$
$4 \times 4 \times 2$	1	5.080	7.675	9.502
$8 \times 8 \times 2$	1	5.572	8.651	10.922
$16 \times 16 \times 2$	1	8.930	14.230	18.275
$32 \times 32 \times 2$	1	9.647	16.556	23.088
Kumar et al. Error! Reference source not found.]	1	5.110	7.612	9.431

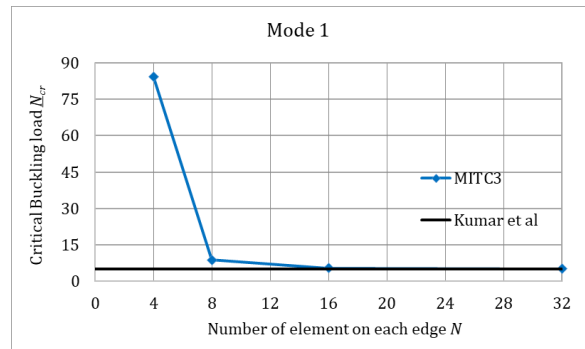


Figure 5. Critical buckling load of CCCC skew plate ( $L/h = 100$ ) with skew angle  $\theta = 30$ .

From the numerical analysis in Table 1, Table 2, and Fig 5, critical buckling load of skew plate with ratio the ratio  $L/h=100$  is subjected to uniform compressive load, mesh  $4 \times 4 \times 2$  to mesh  $32 \times 32 \times 2$ , the difference of skew plate  $\theta = 45^\circ$  to the reference solution is 0,591% - 1550.61%,  $\theta = 60^\circ$  is 0,831% - 1842,98%, and  $\theta = 60^\circ$  to the reference solution is 0,755% - 2078,08%. It shows that the MITC3 elements converge to the reference solution in each skew angle. At the fine mesh, skew plate  $\theta = 45^\circ$  has a smaller difference to the reference solution.

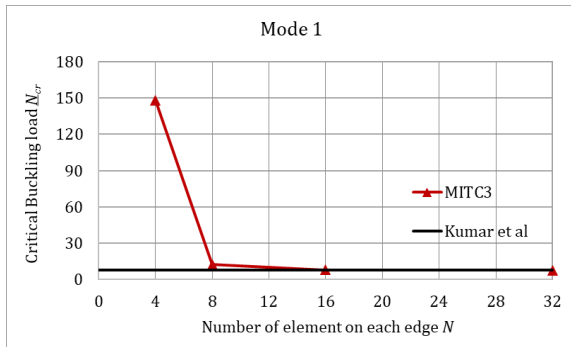


Figure 6. Critical buckling load of CCCC skew plate ( $L/h = 100$ ) with skew angle  $\theta = 60$ .

Fig. 6 indicates that the MITC3 elements converge to the reference solution. in fine mesh, mode 1 skew plate  $\theta = 60^\circ$  has bigger critical buckling than  $\theta = 45^\circ$ , the difference is 2.595. In addition, the skew plate with  $\theta = 60$  has a bigger difference to the reference than  $\theta = 45$ .

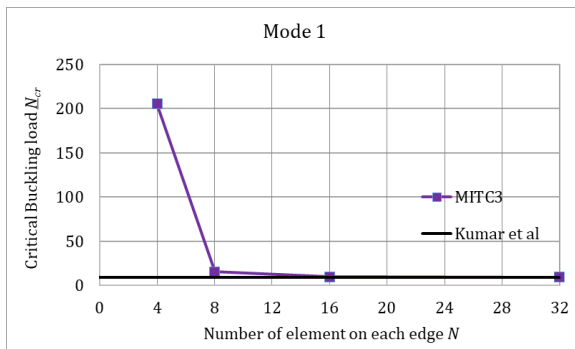


Figure 7. Critical buckling load of CCCC skew plate ( $L/h = 100$ ) with skew angle  $\theta = 60$ .

Fig. 7 represents that a plate with skew angle  $\theta = 75^\circ$  has a bigger critical buckling load than  $\theta = 60^\circ$ , the difference of critical buckling load between  $\theta = 75^\circ$  and  $\theta = 45^\circ$  is 1,827. The unique result is that  $\theta = 75^\circ$  has a smaller difference to the reference solution than  $\theta = 60^\circ$ , From the three skew angles, it is obtained that  $\theta = 60^\circ$  has the largest difference to the reference solution than  $\theta = 45^\circ$ , and  $\theta = 75^\circ$ .

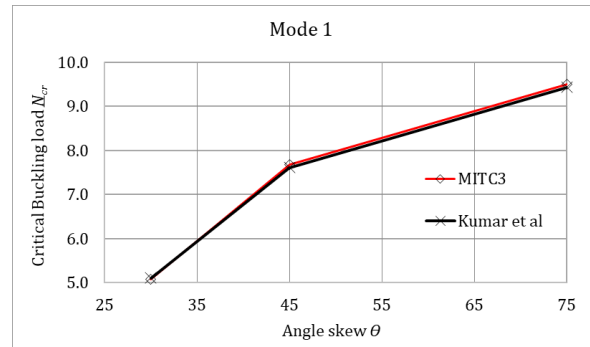


Figure 8. Critical buckling load of CCCC skew plate ( $L/h = 100$ ) according to skew angle.

From Fig 8, it can be seen the effect of increasing the skew angle on the value of the critical buckling load, the skew plate with a ratio of  $L/h = 100$ , the greater the skew angle, the greater the value of the critical buckling load. Another result is that the skew angle  $\theta = 45^\circ$  has the smallest difference to the reference solution.

Table 3. Critical buckling load  $N_{cr}$  of CCCC skew plate with  $L/h = 1000$ .

$N \times N \times 2$	Mode number	$\theta = 45$
$4 \times 4 \times 2$	1	7248.104
$8 \times 8 \times 2$	1	168.136
$16 \times 16 \times 2$	1	13.940
$32 \times 32 \times 2$	1	5.806

Table 4. The first five non-dimensional critical buckling load  $N_{cr}$  of CCCC skew plate with  $L/h = 1000$ .

$N \times N \times 2$	Mode number	$\theta = 45$
$32 \times 32 \times 2$	1	5.806
	2	6.442
	3	11.200
	4	12.304
	5	15.582

Table 5. Critical buckling load  $N_{cr}$  of CCCC skew plate with  $L/h = 1000$ .

$N \times N \times 2$	Mode number	$\theta = 60$
$4 \times 4 \times 2$	1	13492.496
$8 \times 8 \times 2$	1	297.078
$16 \times 16 \times 2$	1	21.155
$32 \times 32 \times 2$	1	8.554

Table 6. The first five non-dimensional critical buckling load  $N_{cr}$  of CCCC skew plate with  $L/h = 1000$ .

$N \times N \times 2$	Mode number	$\theta = 60$
$32 \times 32 \times 2$	1	8.554
	2	9.796
	3	16.930
	4	20.622
	5	23.610

Table 7. Critical buckling load  $N_{cr}$  of CCCC skew plate with  $L/h = 1000$ .

$N \times N \times 2$	Mode number	$\theta = 75$
$4 \times 4 \times 2$	1	19014.590
$8 \times 8 \times 2$	1	431.685
$16 \times 16 \times 2$	1	29.349
$32 \times 32 \times 2$	1	10.769

Table 8. The first five non-dimensional critical buckling load  $N_{cr}$  of CCCC skew plate with  $L/h = 1000$ .

$N \times N \times 2$	Mode number	$\theta = 75$
$32 \times 32 \times 2$	1	10.769
	2	12.713
	3	21.547
	4	29.076

$N \times N \times 2$	Mode number	$\theta = 75$
	5	31.718

From the analysis in tables 4 – 8, MITC3 elements converge to the reference solution but there is a large value gap between the coarse and fine mesh. when the  $L/h$  ratio gets larger, the MITC3 element requires a finer mesh to achieve convergence, in which case the element must be able to qualify as a Kirchhoff plate. where the element must be able to eliminate the effect of shear as the plate gets thinner.

Furthermore, the analysis obtained that increasing the skew angle  $\theta$  and the ratio of  $L/h$  caused an increase in the value of critical buckling load.

## 6. CONCLUSION

Conducting a buckling analysis in the case of a skew plate using the MITC3 element, the results show that the MITC3 element convergence to the reference solution at each skew angle, and in the case of ratio plates of  $L/h = 100$  and  $L/h = 1000$ . Critical buckling load value depends on length to width ratios  $L/h$  and skews angles  $\theta$ , increasing the  $L/h$  and  $\theta$  ratio caused an increase in the value of critical buckling load. We conclude MITC3 element can be used to solve the eigenvalue problem.

## REFERENCES

- [1] Y. Lee, P. S. Lee, and K. J. Bathe, "The MITC3+ shell element and its performance," *Computers and Structures*, vol. 138, pp. 12–23, 2014, doi: 10.1016/j.compstruc.2014.02.005.
- [2] P. S. Lee and K. J. Bathe, "Development of MITC isotropic triangular shell finite elements," *Computers and Structures*, vol. 82, no. 11–12, pp. 945–962, 2004, doi: 10.1016/j.compstruc.2004.02.004.

- [3] K. -J Bathe and E. N. Dvorkin, "A formulation of general shell elements—the use of mixed interpolation of tensorial components," *International Journal for Numerical Methods in Engineering*, vol. 22, no. 3, pp. 697–722, 1986, doi: 10.1002/nme.1620220312.
- [4] E. N. Dvorkin and K. J. Bathe, "A continuum mechanics based four-node shell element for general nonlinear analysis," *Engineering Computations*, vol. 1, no. 1, pp. 77–88, 1984, doi: 10.1108/eb023562.
- [5] A. M. Katili, I. J. Maknun, I. Wulandari, and I. Katili, "Theoretical equivalence and numerical performance of T3s and MITC3 plate finite elements," *Structural Engineering and Mechanics*, vol. 69, no. 5, pp. 527–536, 2019, doi: 10.12989/sem.2019.69.5.527.
- [6] B. C. M Wang, K. M. Liew, and W. A. M Alwis, "BUCKLING OF SKEW PLATES AND CORNER CONDITION FOR SIMPLY SUPPORTED EDGES."
- [7] A. Kumar, S. K. Panda, and R. Kumar, "Buckling behaviour of laminated composite skew plates with various boundary conditions subjected to linearly varying in-plane edge loading," *International Journal of Mechanical Sciences*, vol. 100, pp. 136–144, Jul. 2015, doi: 10.1016/j.ijmecsci.2015.06.018.
- [8] F. T. Wong, Erwin, A. Richard, and I. Katili, "Development of the DKMQ Element for Buckling Analysis of Shear-deformable Plate Bending," *Procedia Engineering*, vol. 171, pp. 805–812, 2017, doi: 10.1016/j.proeng.2017.01.368.
- [9] J. N. Reddy, "J. N. Reddy Mechanics of Laminated Composite Plates and Shells Theory and Analysis, Second Edition 2003." pp. 1–855, 2007. [Online]. Available: [https://books.google.com/books?id=eUr\\_AJiGRcC](https://books.google.com/books?id=eUr_AJiGRcC)
- [10] H. Nguyen-Xuan, L. v. Tran, T. Nguyen-Thoi, and H. C. Vu-Do, "Analysis of functionally graded plates using an edge-based smoothed finite element method," *Composite Structures*, vol. 93, no. 11, pp. 3019–3039, 2011, doi: 10.1016/j.compstruct.2011.04.028.



